Journal of Crystal Growth 617 (2023) 127272

Contents lists available at ScienceDirect

Journal of Crystal Growth

journal homepage: www.elsevier.com/locate/jcrysgro

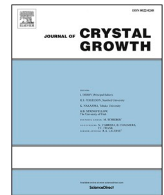

Growth of non-polar m-plane GaN pseudo-substrates by Molecular beam epitaxy

Amalia Fernando-Saavedra [a,*], Steven Albert [a], Ana Bengoechea-Encabo [a], Achim Trampert [b], Mengyao Xie [c], Miguel A. Sanchez-Garcia [a], Enrique Calleja [a]

[a] ISOM and Dept. Ingeniería Electrónica, ETSI Telecomunicación, Universidad Politécnica de Madrid, Av. Complutense 30, Ciudad Universitaria, 28040 Madrid, Spain
[b] Paul-Drude-Institut für Festköperelektronik, Hausvogteiplatz 5-7, 10117 Berlin, Germany
[c] Tianrui Semiconductor Materials (Suzhou) Ltd.co., the Third Zone of Datong rd. 20, Suzhou New District, 215151 Suzhou, PR China

ARTICLE INFO

Communicated by: Maria Hilse

Keywords:
A1.Etching
A3.Molecular beam epitaxy
A3.Selective epitaxy
B1.Nitrides
B2.Semiconducting III-V materials

ABSTRACT

Non-polar m-plane GaN films were grown by Plasma Assisted Molecular Beam Epitaxy on γ-$LiAlO_2$ (1 0 0) substrates by a controlled coalescence of GaN nanocolumns obtained by a two-step process including a top-down nanopillars etching from a GaN buffer and a subsequent bottom-up overgrowth. Transmission electron microscopy data show a significant reduction of extended defects density in the coalesced film as compared to the initial GaN buffer, most likely due to a filter effect by the regrowth process on the nanopillars inclined walls. Low temperature photoluminescence spectra back this reduction by a strong intensity decrease of the stacking faults fingerprint emission peaks, while a very intense donor-bound excitonic emission at 3.472 eV, 2.8 meV wide, becomes dominant.

1. Introduction

III-nitride semiconductors have unique properties that make them one of the most adequate materials family to develop opto-electronic devices. Typically, III-nitrides are heteroepitaxially grown on sapphire, SiC and Si(1 1 1) with a high density of structural defects, such as stacking faults (SFs), inversion domain boundaries (IDBs) and threading dislocations (TDs), due to thermal and lattice mismatch, surface morphology and polarity changes. These structural defects disrupt the crystal periodicity having a detrimental effect on the optical and transport (mobility) material properties. Different approaches aiming at quality upgrade have been proposed in the past, such as buffer layers [1] to accommodate lattice mismatch, or special growth techniques such as epitaxial lateral overgrowth (ELOG) by Metalorganic Vapour-Phase Epitaxy (MOVPE) [2], that alleviate this problem.

Another potential problem in III-nitride-based devices relates to the presence of a strong internal polarization field along the c-polar direction that can be detrimental in Laser Diodes (LD) and Light Emitting Diodes (LED), or beneficial, like in High Electron Mobility Transistors (HEMTs). A large number of groups are involved in non-polar and semi-polar LD and LED research, both in UV and visible regions to reduce or avoid the internal electric field. Growth of non-polar m-plane materials on lithium aluminate substrates [3] and a-plane GaN on r-plane sapphire [4–7] was achieved. However, GaN growth on such semi-polar and non-polar substrates may result in rough surface morphologies and a higher density of defects (SFs and TDs) [8]. Although, InGaN/GaN QW LDs grown on non-polar GaN m-plane free-standing substrates have been realized [9,10], nowadays these substrates are limited in size and high in cost.

An alternate approach to reduce defect density is the use of pseudo-substrates, namely, thick films grown on cheap substrates with good enough quality for further growth with the possibility to tailor the in-plane lattice constants. Related works were recently published on semi-polar and non-polar a-plane oriented GaN obtained by overgrowth on a template of self-organized nanocolumns [11], or ordered patterns of microstructures [12], both by epitaxial lateral overgrowth (ELOG) using MOVPE. A similar approach was addressed by coalescence of selectively grown nanocrystals by plasma-assisted molecular beam epitaxy (PAMBE) using colloidal lithography [13] which does not produce ordered arrays. GaN nanocrystals offer a much higher structural quality than their films counterpart due to their very low defect density and strain free features [14,15]. Ordered nanocolumns (NCs) can be either grown with the help of a patterned nanohole mask (typical SAG method) [15,16], by a top-down etching process using a metal mask

* Corresponding author.
E-mail address: amalia.fsaavedra@fundetel.upm.es (A. Fernando-Saavedra).

https://doi.org/10.1016/j.jcrysgro.2023.127272
Received 16 March 2023; Received in revised form 11 May 2023; Accepted 16 May 2023
Available online 25 May 2023
0022-0248/© 2023 Elsevier B.V. All rights reserved.

[17], or by a combination of both methods [18] where first nanopillars (NPs) are etched from a GaN buffer and further overgrown. The versatility in fabrication and outstanding properties make ordered GaN NCs very appealing not only as active part of nanodevices, but also as template material for further epitaxial growth.

This work addresses the growth of non-polar m-plane GaN pseudo-substrates on γ-$LiAlO_2$ (1 0 0) (LAO) by a combination of an ordered pattern of etched NPs and a subsequent GaN overgrowth by PAMBE until coalescence into a film is achieved. LAO has a tetragonal structure with lattice constants a = b = 5.1687 Å and c = 6.2679 Å. So, the use of LAO substrates allows the growth of m-plane oriented GaN due to the small lattice mismatch between them (0.3% and 1.7% along [11–20] and [0001] directions, respectively) [19] and moreover, it has been proposed as an intermediate for achieving free-standing GaN via a self-separation process [20,21]. The morphological evolution of the overgrown NPs is shown on two arrays with different designs. Transmission electron microscopy (TEM) characterization shows a defect density decrease upon GaN NCs coalescence with no measurable tilt or twist between NCs. Indeed, SFs and TDs, already present in the GaN buffer grown on LAO (and therefore, also in the etched NPs) are efficiently filtered between NPs and partially filtered above them. Photoluminescence (PL) measurements point to this SFs reduction in terms of a strong intensity decrease of various SFs fingerprint emission peaks, while a very intense, 2.8 meV wide, donor-bound excitonic emission (D^0X) at 3.472 eV, becomes dominant. Overall, the results prove that this approach is a promising path for achieving high quality m-plane GaN pseudo-substrates.

2. Experimental section

A GaN buffer was grown on a quarter of 2-inch commercial LAO wafer (MTI Corporation) substrate using a Riber Compact 21 PAMBE system with a rf-plasma source for active nitrogen. The LAO substrate was sequentially cleaned 5 min in acetone, 5 min in isopropanol, dipped in de-ionized (DI) water and dried with N_2. The substrate was loaded into the PAMBE system to degas for 30 min at 300 ºC in the introduction chamber and for 5 min at 500 °C in the growth chamber. A Ga wetting layer was deposited for 5 s at 500 °C (equivalent to 2.7 monolayers in GaN units) then the GaN growth was performed with a Ga flux of 8.5 nm/min and an active N flux of 5 nm/min following two steps: first at 580 °C for 13 min, then at 770 ºC for 3 h [19].

Fig. 1 shows the sequence of steps to fabricate the pseudo-substrates. GaN NPs were etched on the GaN buffer following the process described in A. Fernando-Saavedra et al. [18] (Fig. 1a). Then, GaN overgrowth proceeded for 15 h, checked ex situ by scanning electron microscopy (SEM) at different time stages until coalescence occurred, with a Ga flux of 16.5 nm/min and N of 3 nm/min at 850 °C (Fig. 1b and 1c).

Samples were characterized by SEM using a FEI Inspect F50 system, by low temperature photoluminescence (LT-PL) using a He-Cd laser (325 nm @ 13 mW power excitation) and by transmission electron microscopy (TEM) using a Jeol-JEM 2100F operating at 200 kV. The GaN buffer cross-sectional lamella were prepared by mechanical pre-thinning and final argon ion milling to achieve electron transparency. For GaN coalesced film, a focusing ion beam (FIB) milling processes along [0001] and [11–20] orientations were used.

3. Results and discussion

A non-polar m-plane GaN buffer, 900 nm thick (estimated by growth conditions and confirmed by TEM measurements) grown on a LAO substrate is shown in Fig. 2. A cross-sectional TEM image along the [11–20] direction shows dark lines crossing the entire epilayer normal to the surface, related to a high density of extended defects identified as SFs by High-Resolution TEM (HRTEM). This is in good agreement with the stripes connecting the bright spots along the [0001] direction in the Selected-Area Electron Diffraction (SAED) pattern [22] shown in Fig. 2c, that is related with basal plane disorder.

Two square arrays, well oriented towards the [0001] and [11–20] directions (see *supporting information*), of NPs with truncated cone shape were etched on the GaN buffer. Sample A with NPs pitch of 600 nm with upper/lower diameters of 250 nm and 400 nm respectively and 500 nm height (Fig. 3a) and Sample B with NPs pitch of 300 nm and upper/lower diameters of 150 nm and 250 nm respectively and same height as in Sample A.

Fig. 3b to 3f show the morphology evolution of Sample A during overgrowth, checked in sequential periods of 1 h, from an etched NP to a GaN NC with fully developed m- and c-planes. NPs top and sidewalls surfaces are rough due to the etching process by inductively coupled plasma (ICP). During the overgrowth the NPs evolve into a rectangular shape involving c-, a- and m-planes. Energy minimization conditions lead to a perfect hexagonal NC with full m-plane sidewalls as shown in Fig. 3f (hexagonal prism lying on the m-plane sidewall).

After the growth steps corresponding to images in Fig. 3, overgrowth was continued for up 15 h to achieve a GaN film by NCs coalescence. The morphology evolution at time intervals of 1, +5 (6), and + 9 (15) hours of samples A and B are shown in Fig. 4. After 1 h growth NCs in both samples still have some semi-polar facets (more pronounced in Sample A, as shown in Fig. 3b).

At this point it should be noticed that in III-nitrides nanostructures the preferential growth direction (thus, the growth rate) is always along the [0001] direction [23,24], that, in this case, is parallel to the surface, what explains the NCs prismatic shape. However, Fig. 3 shows that neither c- nor m-planes are fully formed after 1 h growth, so that the growth rate differences already mentioned should be considered when the NCs hexagonal facets are fully formed (or at least the c-planes). Then, the coalescence of formed NCs depends mainly on the distance between neighbouring NPs along both in-plane [11–20] and [0001] directions. In this case, this distance is much larger in sample A than that in Sample B (200 and 50 nm at the NPs bottom respectively).

NCs coalescence in sample A is achieved along the [0001] direction after 6 h growth, while coalescence along [11–20] direction takes much longer, i.e. 15 h, leaving visible V-shaped trenches. On the other hand, in Sample B coalescence along [0001] and [11–20] directions occurs faster (shorter distance between neighbouring NPs) leaving visible V-shaped trenches after 6 h that smooth out after 15 h yielding a rather flat surface. Indeed, a similar result would also be obtained in Sample A after a much longer time than 15 h, so, for practical purposes, the NPs diameter and pitch should be carefully selected to reduce the time for the

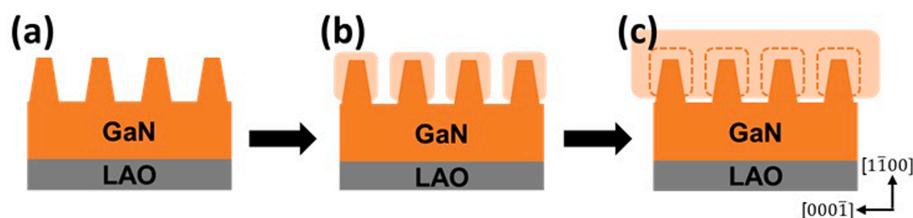

Fig. 1. Sketch of the fabrication process: (a) GaN NPs etched on a GaN buffer grown on LAO, (b) GaN overgrowth until (c) GaN coalescence where the dash-orange shapes show the shape of the GaN overgrowth at the beginning.

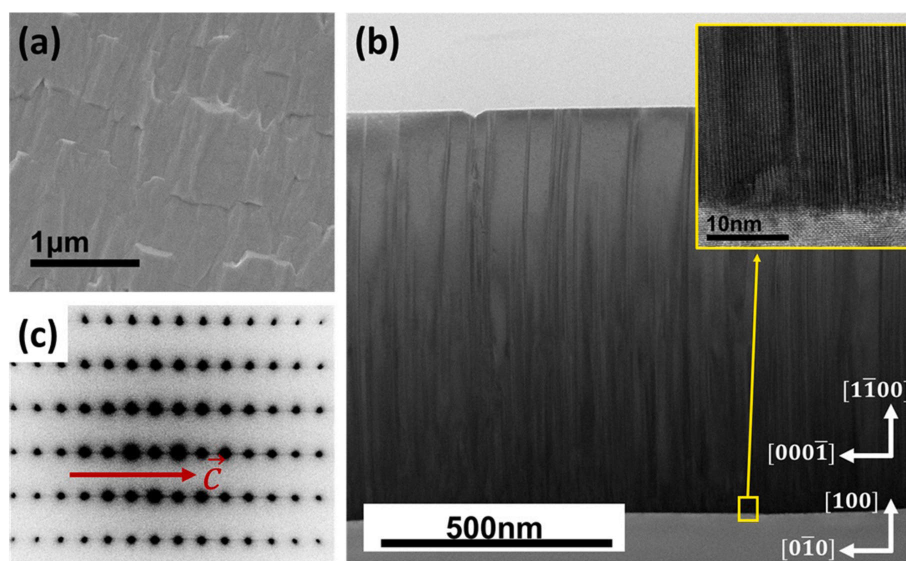

Fig. 2. (a) SEM top view image of the GaN buffer, (b) cross-sectional Bright Field Scanning TEM (BF-STEM) image of the GaN buffer along the [11–20] direction where the inset shows a HRTEM image of the GaN buffer at the interface and (c) SAED pattern of the GaN buffer along the [11–20] direction.

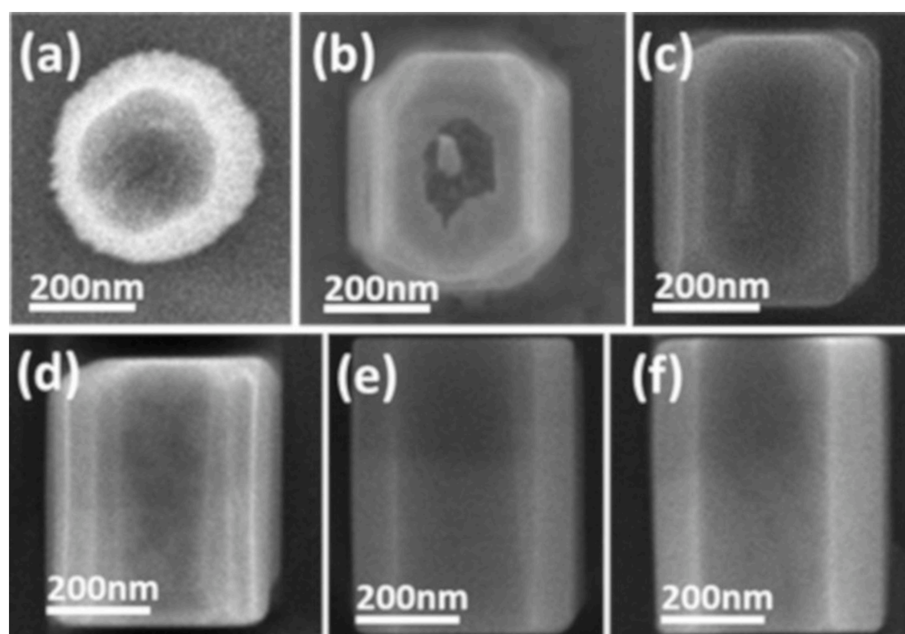

Fig. 3. Top view SEM images (Sample A) of (a) etched NPs, (b-f) GaN overgrowth checked at sequential periods of 1 h.

coalescence, while avoiding residual strain (not too big diameters).

Fig. 5 shows the growth rates along [0001] and [11–20] directions for NCs, measured as the NC in-plane lengths in Sample A from two hours growth on, being 4 times faster along [0001] direction than along [11–20] direction (during the first 5 h of growth). The slope change observed for the length along the [11–20] direction after 5 h growth can be interpreted as due to coalescence along the [0001] direction (growth stops along this direction), so that in-plane growth proceeds only along the [11–20] direction.

Fig. 6 shows LT- PL spectra taken from the GaN buffer, the etched NPs and the coalesced film in Sample B. The spectrum of the GaN buffer (green double dot dashed) is blue shifted by biaxial compressive strain, as expected when growing GaN on LAO [25]. The dominant peak is located at 3.348 eV ($I_{2'}$) identified as intrinsic I_2 SFs family [26,27], together with another two weaker peaks at 3.437 eV ($I_{1'}$) and 3.494 eV (D^0X') identified as intrinsic I_1 SFs family [27,28] and the D^0X emission respectively. Upon NPs etching strain relaxes and the whole spectrum red-shifts to the unstrained positions at 3.332 eV (I_2), 3.410 eV (I_1) and 3.472 eV (D^0X) (red dashed line). The dominant SF lines are typically observed in nonpolar GaN grown on LAO [20,23] and agree with TEM data in Fig. 2b. Finally, the PL spectrum from the coalesced film is clearly dominated by the D^0X emission at 3.472 eV (black solid) with a 2.8 meV linewidth, while in contrast SFs signatures become weak. In addition, the appearance of $I_{2'}$, $I_{1'}$ and D^0X' at the same position as in the GaN buffer, most likely arise from the remaining buffer through some exposed areas formed by defective masking, or incomplete coalesced layers between stripes (see *supporting information*).

Structural details of the GaN coalesced films were studied by TEM. Fig. 7a, 7b show cross-sectional TEM images along the [11–20] direction and Fig. 7c, 7d along the [0001] direction of Samples A and B respectively, where the white dashed and pointed shapes represent the initial etched NPs as truncated cones. The coalesced films are about 1.15 μm

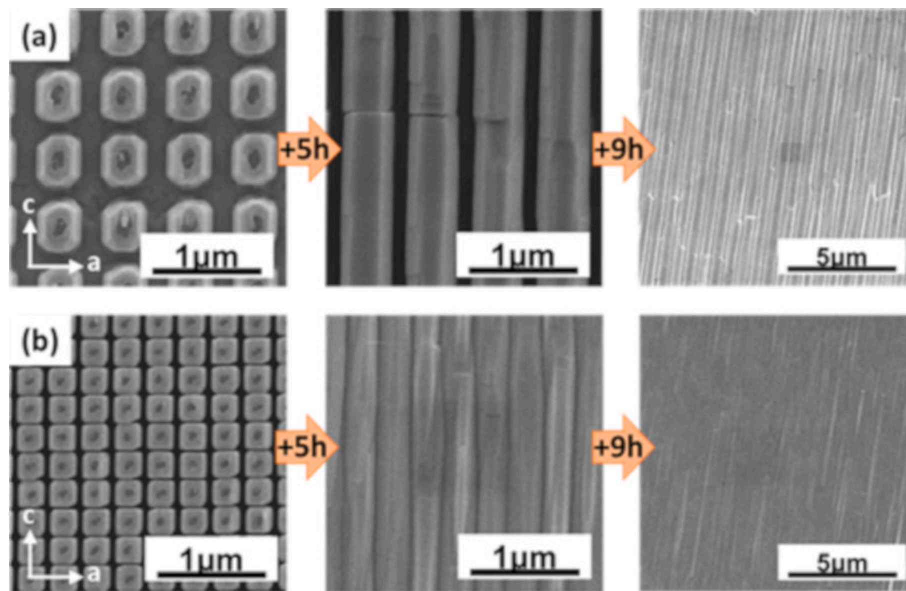

Fig. 4. Top view SEM images of the GaN overgrowth evolution with time on: (a) sample A and (b) sample B.

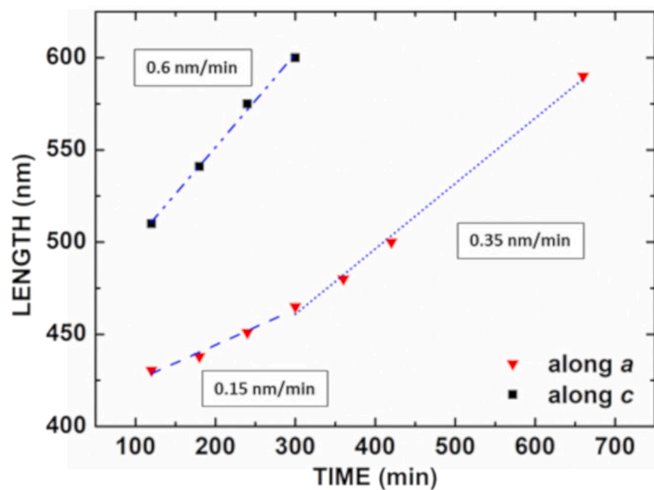

Fig. 5. In-plane NCs lengths (±10 nm) along [0001] (polar, black squares) and [11–20] (non-polar, red triangles) directions in sample A starting to be measured after 2 h growth. The different growth rates are also indicated.

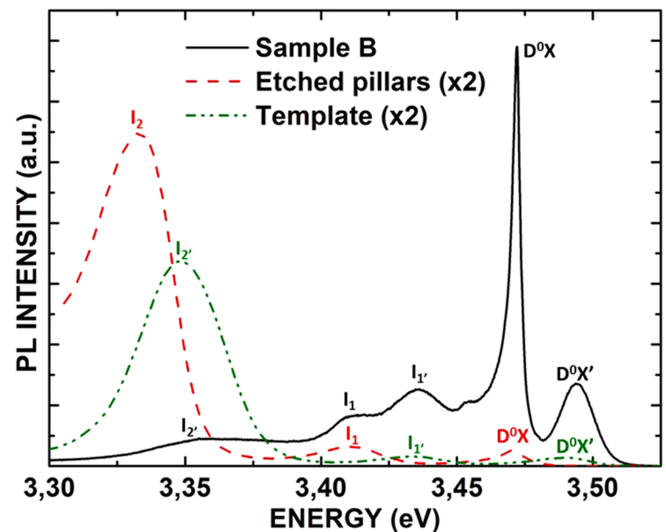

Fig. 6. LT-PL spectra of the GaN buffer (green double dot dashed); etched pillars (red dashed) and coalesced film of sample B (black solid).

thick and do not show domains with measurable tilt or twist measured by local, spatially resolved SAED and HRTEM (see *supporting information*).

Considering first Sample A, the black lines running perpendicular to the top surface (Fig. 7a), identified as SFs, show up with high density within the remaining buffer and the etched NPs, but barely observed in between NPs and with lower density above them. White arrows point to the coalescence lines between nanocrystals along the [0001] direction, identify as intrinsic I_2 SFs by TEM (see *supporting information*). Fig. 7c shows TEM images along the [0001] direction in Sample A where the dark lines, very dense within the remaining buffer, and barely seen above NPs are identified as TDs (in the basal planes). It seems that dislocations are filtered in sample A when GaN overgrowth proceeds on the NPs. This filtering effect on extended defects was already commented in [18] occurring when various facets are formed during crystal regrowth on the NPs truncated cone inclined walls. Fig. 7c also shows the nanocrystals coalescence along the [11–20] direction, leaving voids because of the mentioned lower growth rate along this direction and the high NPs pitch.

In Sample B results from TEM analysis (Fig. 7b and 7d) are basically similar but for a few differences, namely, a lesser filtering effect on SFs and TDs that run above NPs and the voids between nanocrystals which are narrower due to the smaller NPs pitch. The observed difference in filtering effects (actually, there are less TDs and SFs above NPs in Sample A) may be dependent on the specific truncated cone shape (different angle of the sidewalls) and pitch of NPs, though there is no in-depth study of it yet. However, although experimental results may suggest a stronger filtering effect in NPs arrays with larger pitch, the much longer times needed for full coalescence have to considered for practical reasons.

4. Conclusions

High quality non-polar m-plane GaN films were obtained by controlled coalescence of GaN NCs made on a GaN/LAO substrate, following a top-down etching to produce ordered NPs and a subsequent overgrowth by PAMBE.

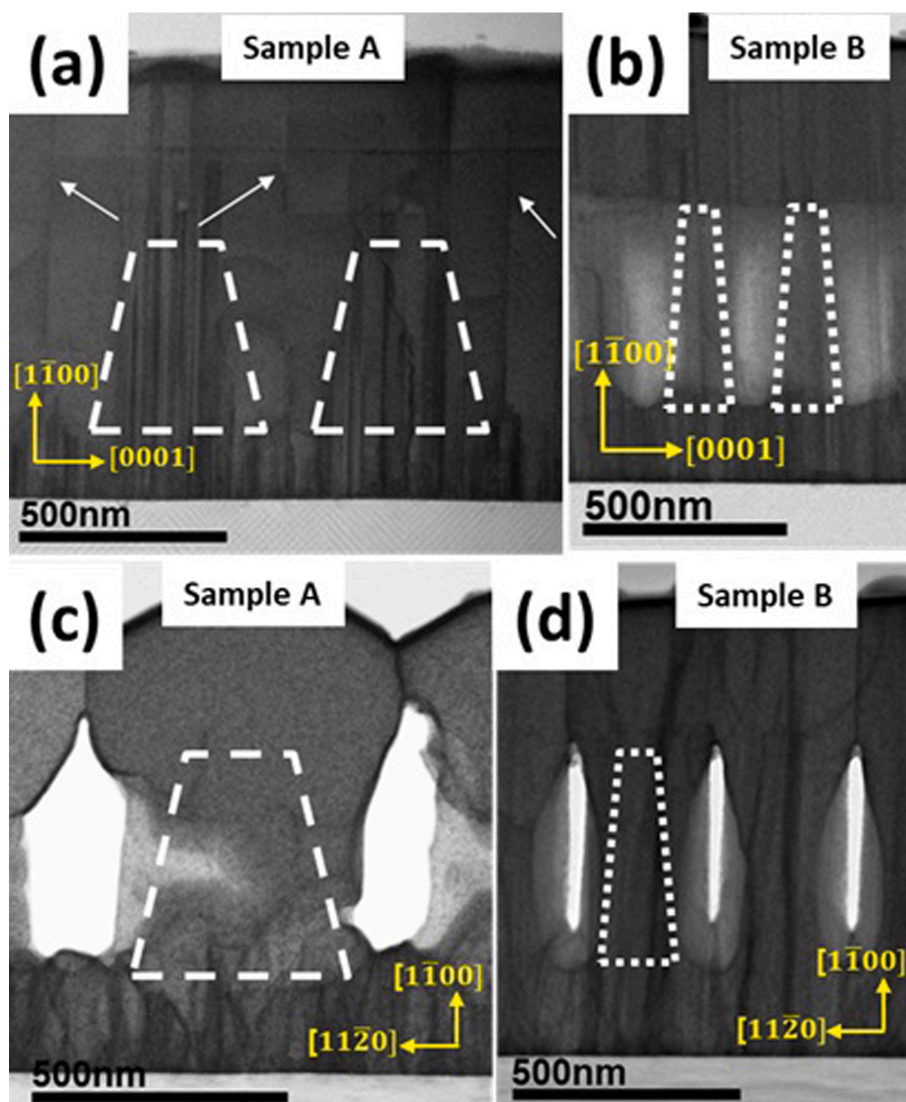

Fig. 7. Cross-sectional TEM images along direction [11–20] of: (a) sample A and (b) sample B and along direction [0001] of: (c) sample A and (b) sample B. The white dashed and pointed lines show the shape of the etched NPs in both samples.

TEM measurements reveal that SFs and TDs present in the buffer layer and the etched NPs may be efficiently filtered by facet formation upon crystalline regrowth at the NPs inclined walls, with an efficiency that apparently depends on the NPs specific truncated cone shape. The significant reduction of extended defects observed by TEM was also revealed by PL measurements, where a D^0X emission with a line width of 2.8 meV becomes dominant in the coalesced film, with just traces of SFs. This process may be applicable to any III-nitride buffer layer grown on LAO or any other non-polar substrate, like r-sapphire.

In addition, it was determined that a square arrangement of NPs, well oriented towards the [0001] and [11–20] directions, apparently helps uniform coalescence when the NPs diameter and pitch are selected to balance the faster growth rate along the [0001] direction.

CRediT authorship contribution statement

Amalia Fernando-Saavedra: Investigation, Resources, Methodology, Visualization, Writing – original draft. **Steven Albert:** Investigation, Methodology. **Ana Bengoechea-Encabo:** Investigation, Resources, Methodology, Writing – review & editing. **Achim Trampert:** Investigation. **Mengyao Xie:** Supervision, Funding acquisition. **Miguel A. Sanchez-Garcia:** Supervision, Project administration, Writing – review & editing. **Enrique Calleja:** Supervision, Funding acquisition, Writing – review & editing.

Declaration of Competing Interest

The authors declare the following financial interests/personal relationships which may be considered as potential competing interests: [Enrique Calleja Pardo reports financial support was provided by LanRui Semiconductor Materials Ltd.co. Miguel Angel Sanchez Garcia and Enrique Calleja Pardo reports financial support was provided by Tianrui Semiconductor Materials Ltd.co. Achim Trampert reports financial support was provided by European Regional Development Fund. Amalia Fernando-Saavedra has patent Non-polar III-Nitride binary and ternary materials, method for obtaining thereof and uses licensed to EP 3 812 487 A1.].

Data availability

No data was used for the research described in the article.

Acknowledgment

The Spanish team wishes to acknowledge the financial support by LanRui Semiconductor Materials (Shanghai) Ltd.co and Tianrui Semiconductor Materials Ltd.co. Also, to the Institute of Optoelectronic Systems and Microtechnology (ISOM) among the Singular Scientific and Technical Infrastructures (ICTS) in Spain (Micronanofabs). A. Trampert acknowledges financial support by the European Union and the state of Berlin within the frame of the European Regional Development Fund (ERDF), project number 2016011843.

Appendix A. Supplementary material

Supplementary data to this article can be found online at https://doi.org/10.1016/j.jcrysgro.2023.127272.

References

[1] S. Nakamura, GaN Growth Using GaN Buffer Layer, Jpn. J. Appl. Phys. 30 (1991) L1705–L1707.
[2] O.-H. Nam, M.D. Bremser, T.S. Zheleva, R.F. Davis, Lateral epitaxy of low defect density GaN layers via organometallic vapor phase epitaxy, Appl. Phys. Lett. 71 (18) (1997) 2638–2640.
[3] P. Waltereit, O. Brandt, A. Trampert, H.T. Grahn, J. Menniger, M. Ramsteiner, M. Reiche, K.H. Ploog, Nitride semiconductors free of electrostatic fields for efficient white light-emitting diodes, Nature 406 (6798) (2000) 865–868.
[4] H.M. Ng, Molecular-beam epitaxy of GaN/$Al_xGa_{1-x}N$ multiple quantum wells on R-plane $(10\bar{1}2)$ sapphire substrates, Appl. Phys. Lett. 80 (2002) 4369-4371.
[5] H.M. Ng, A. Bell, F.A. Ponce, S.N.G. Chu, Structural and optical characterization of nonpolar GaN/AlN quantum wells, Appl. Phys. Lett. 83 (4) (2003) 653–655.
[6] T. Paskova, Development and prospects of nitride materials and devices with nonpolar surfaces, Phys. stat. sol. (b) 245 (6) (2008) 1011–1025.
[7] J.S. Speck, S.F. Chichibu, Nonpolar and Semipolar Group III Nitride-Based Materials, MRS Bull. 34 (5) (2009) 304–312.
[8] P. Vennéguès, Defect reduction methods for III-nitride heteroepitaxial films grown along nonpolar and semipolar orientations, Semicond. Sci. & Technol. 27 (2012), 024004.
[9] R.M. Farrell, E.C. Young, F. Wu, S.P. DenBaars, J.S. Speck, Materials and growth issues for high-performance nonpolar and semipolar light-emitting devices, Semicond. Sci. & Technol. 27 (2) (2012) 024001.
[10] K. Okamoto, H. Ohta, D. Nakagawa, M. Sonobe, J. Ichihara, H. Takasu, Dislocation-Free m-Plane InGaN/GaN Light-Emitting Diodes on m-Plane GaN Single Crystals, Jpn. J. Appl. Phys. 45 (No. 45) (2006) L1197–L1199.
[11] J. Bai, Y. Gong, K. Xing, X. Yu, T. Wang, Efficient reduction of defects in (11–20) non-polar and (11–22) semi-polar GaN grown on nanorod templates, Appl. Phys. Lett. 102 (2013), 101906.
[12] L. Jiu, Y. Gong, T. Wang, Overgrowth and strain investigation of (11–20) non-polar GaN on patterned templates on sapphire, Sci. Rep. 8 (2018) 9898.
[13] S. Albert, A. Bengoechea-Encabo, J. Zuniga-Perez, P. de Mierry, P. Val, M. A. Sanchez-Garcia, E. Calleja, Selective area growth of GaN nanostructures: A key to produce high quality (11–20) a-plane pseudo-substrates, Appl. Phys. Lett. 105 (2014), 091902.
[14] E. Calleja, M.A. Sánchez García, F.J. Sánchez, F. Calle, F.B. Naranjo, E. Muñoz, U. Jahn, H.K. Ploog, Luminescence properties and defects in GaN nanocolumns grown by molecular beam epitaxy, Phys. Rev. B 62 (2000) 16826.
[15] K. Kishino, T. Hoshina, S. Ishizawa, A. Kikuchi, Selective-area growth of GaN nanocolumns on titanium-mask-patterned silicon (111) substrates by RF-plasma-assisted molecular-beam epitaxy, Electron. Lett 44 (2008) 819–821.
[16] A. Bengoechea-Encabo, F. Barbagini, S. Fernandez-Garrido, J. Grandal, J. Ristic, M. A. Sanchez-Garcia, E. Calleja, U. Jahn, E. Luna, A. Trampert, Understanding the selective area growth of GaN nanocolumns by MBE using Ti nanomasks, J. Cryst. Growth 325 (1) (2011) 89–92.
[17] R. Debnath, J.Y. Ha, B. Wen, D. Paramanik, A. Motayed, M.R. King, A.V. Davydov, Top-down fabrication of large-area GaN micro- and nanopillars, J. Vac. Sci. Technol. B 32 (2014), 021204.
[18] A. Fernando-Saavedra, S. Albert, A. Bengoechea-Encabo, D. Lopez-Romero, M. Niehle, S. Metzner, G. Schmidt, F. Bertram, M.A. Sánchez-García, A. Trampert, J. Christen, E. Calleja, Ordered arrays of defect-free GaN nanocolumns with very narrow excitonic emission line width, J. Cryst. Growth 525 (2019), 125189.
[19] Y.J. Sun, O. Brandt, K.H. Ploog, Growth of M-plane GaN films on γ-$LiAlO_2$ (100) with high phase purity, J. Vac. Sci. Technol. B 21 (2003) 1350–1356.
[20] E. Richter, C.h. Hennig, U. Zeimer, M. Weyers, G. Tränkle, P. Reiche, S. Ganschow, R. Uecker, K. Peters, Freestanding two inch c-plane GaN layers grown on (100) γ-lithium aluminium oxide by hydride vapour phase epitaxy, Phys. Stat. Sol. (c) 3 (6) (2006) 1439–1443.
[21] L. Wang, U. Zeimer, E. Richter, C.h. Hennig, M. Herms, M. Weyers, Characterization of free standing GaN grown by HVPE on a $LiAlO_2$ substrate, Phys. Stat. Sol. (a) 203 (7) (2006) 1663–1666.
[22] T.Y. Liu, A. Trampert, Y.J. Sun, O. Brandt, K.H. Ploog, Microstructure of M-plane GaN epilayers on γ-$LiAlO_2$ by plasma-assisted molecular beam epitaxy, Philos. Mag. Lett. 84 (2004) 435–441.
[23] L. Lymperakis, J. Neugebauer, Large anisotropic adatom kinetics on nonpolar GaN surfaces: Consequences for surface morphologies and nanowire growth, Phys. Rev. B 79 (2009) 241308(R).
[24] A. Bengoechea-Encabo, S. Albert, M.A. Sanchez-Garcia, L.L. López, S. Estradé, J. M. Rebled, F. Peiró, G. Nataf, P. de Mierry, J. Zuniga-Perez, E. Calleja, Selective area growth of a- and c-plane GaN nanocolumns by molecular beam epitaxy using colloidal nanolithography, J. Cryst. Growth 353 (1) (2012) 1–4.
[25] J.W. Gerlach, A. Hofmann, T. Hoeche, F. Frost, B. Rauschenbach, G. Benndorf, High-quality m-plane GaN thin films deposited on γ-$LiAlO_2$ by ion-beam-assisted molecular-beam epitaxy, Appl. Phys. Lett. 88 (2006), 011902.
[26] I. Tischer, M. Feneberg, M. Schirra, H. Yacoub, R. Sauer, K. Thonke, I_2 basal plane stacking fault in GaN: Origin of the 3.32 eV luminescence band, Phys. Rev. B 83 (2011), 035314.
[27] J. Lähnemann, U. Jahn, O. Brandt, T. Flissikowski, P. Dogan, H.T. Grahn, Luminescence associated with stacking faults in GaN, J. Phys. D: Appl. Phys. 47 (2014) 4230001.
[28] P. Corfdir, F. Feix, J.K. Zettler, S. Fernández-Garrido, O. Brandt, Importance of the dielectric contrast for the polarization of excitonic transitions in single GaN nanowires, New J. Phys. 17 (2015), 033040.